Structure and diffusion of boron in amorphous silica: Role of oxygen vacancy related defects

Chin-Lung Kuo and Gyeong S. Hwang*
Department of Chemical Engineering, University of Texas, Austin, Texas 78713, USA
(Received 29 September 2008; revised manuscript received 22 December 2008; published 6 April 2009)

Based on first-principles density-functional calculations, we present the structure and diffusion of boron in amorphous silica, as well as in crystalline silica for comparison purpose. We find that incorporation of a boron atom into the amorphous silica matrix results in various minimum-energy configurations with and without oxygen deficient centers, and also the B-related defects can undergo interconversions at elevated temperatures. While B atoms preferentially remain in the trigonal BO_3 form in amorphous silica, our work shows that B diffusion may require transformation of the immobile BO_3 state to a mobile B state by capturing oxygen vacancy related defects equivalent to an S center, which is a combination of an oxygen vacancy and a trivalent Si defect with an unpaired electron. Considering an energy cost for S center creation, our predicted activation energy of B diffusion is in good agreement with experiments. In addition, the defect-mediated diffusion model can explain the observed correlation of B diffusion and Si self-diffusion in amorphous silica.

DOI: 10.1103/PhysRevB.79.165201 PACS number(s): 61.72.jj, 85.40.Ry

I. INTRODUCTION

Boron penetration through the thin gate oxide from the p^+ poly-Si gate to the channel region becomes a serious obstacle to continuing traditional scaling of complementary metal-oxide-semiconductor (CMOS) devices.[1,2] Several studies have been undertaken to understand mechanisms underlying boron diffusion in oxides. The first model was proposed by Fair based on thermochemical data,[3,4] which assumes B diffusion via peroxy linkage (PL) defects, ≡Si-O-O-Si≡. This model appears plausible if the PL defect exists abundantly because it may interact with B to form the mobile ≡Si-O-B-O-Si≡ complex. Later, based on first-principles calculations Otani and co-workers[5,6] proposed a viable route for B diffusion in α quartz with a predicted barrier of 2.1–2.3 eV, while showing the possible existence of a variety of stable and metastable B configurations. This model explains well the structure and diffusion of B in the crystalline silica network. However, in an amorphous oxide (a-SiO_2) layer, the activation energy of B diffusion has been found to be 3.5–4.0 eV.[4,7,8] The activation energy difference between the crystalline and amorphous cases could be attributed to the fact that the more flexible amorphous network generally yields richer local bonding environments than the crystalline counterpart.

In fact, B diffusion in the amorphous gate oxide exhibits some intricate behaviors, which cannot be explained by the currently available models. For instance, like Si self-diffusion B diffusion has been found to be enhanced by decreasing the oxide layer thickness,[9–11] which might be attributed to SiO pairs and/or their related defects generated at the Si/SiO_2 interface during high-temperature annealing. Earlier experiments[9–12] have also evidenced that both Si self-diffusion and B diffusion are facilitated as B concentration increases in a thin gate oxide, while the presence of B atoms also results in enhancement of SiO pair diffusion.[11] Based on the observations, it was suggested that the enhanced SiO diffusivity might be responsible for the correlated B and Si diffusion.[9–11] In addition, a recent experiment[13] has shown that Si defects, such as $E^/$ centers, generated by ion-implantation lead to increasing B penetration through the thin gate oxide, while it has been theoretically demonstrated that SiO pairs can easily convert to oxygen vacancies in a-SiO_2.[14] This may suggest a possible role of oxygen vacancy related defects in B diffusion in the amorphous oxide matrix, but the underlying mechanism is unclear.

In this paper, we present an atomic-scale model for B diffusion mediated by oxygen vacancy related defects in a-SiO_2 based on first-principles density-functional calculations. We first determine minimum-energy states for B atoms in a-SiO_2, as well as in crystalline α quartz for the sake of comparison. The studies show possible interconversions between B-related defects in a-SiO_2, associated with trivalent Si defects such as S and $E^/$ centers, which is not seen in α quartz. Then, we look at the formation and diffusion of the Si defects and their role in B diffusion in a-SiO_2. This work can assist in better understanding the complex interaction between B atoms and oxygen vacancy related defects as well as the correlated diffusion behavior of Si and B atoms in the thin oxide.

II. COMPUTATIONAL METHODS

All atomic structures and energies reported herein were calculated using first-principles calculations based on spin-polarized density-functional theory (DFT) within the generalized gradient approximation of Perdew and Wang [PW91 (Ref. 15)], as implemented in the well established Vienna *ab initio* simulation package (VASP).[16] Vanderbilt ultrasoft pseudopotentials for core-electron interactions[17] and a plane-wave basis set for valence electron states were employed. A plane-wave cutoff energy of 300 eV was used for *ab initio* molecular dynamics (MD) simulations and 400 eV was used for structural optimization and energetic calculations. The Brillouin-zone integration was performed using a $(2\times2\times2)$ mesh of k points in the scheme of Monkhorst-Pack, sufficient for the disordered SiO_2 systems considered in this work. We checked carefully the convergence of atomic configurations and relative energies with respect to the plane-wave cutoff energy and the k-point mesh size. All atoms

were fully relaxed using the conjugate gradient method until residual forces on constituent atoms become smaller than 5×10^{-2} eV/Å. Diffusion pathways and barriers were computed using the nudged elastic band method (NEBM). In applying this method, sixteen intermediate images were used to determine the converged minimum-energy paths between adjacent local energy minimums. In calculating a charged defect, a homogeneous background charge is included to maintain the overall charge neutrality in the periodic supercell. To account for the coulomb energy between the charged defect and the background charge, a monopole correction is made to the total energy of the charged system. Assuming a pointlike charge defect in a cubic supercell with a lattice constant of 10.108 Å, the monopole correction is estimated to be approximately 0.53 eV based on a dielectric constant of 3.8 for SiO_2.

Bulk crystalline SiO_2 (α quartz) is modeled using a 72-atom supercell with lattice constants of a=4.917 Å and c =5.430 Å. Due to flexible Si-O-Si linkages, the supercell size appears to be sufficient for describing the structure and diffusion of an inserted atom with no significant interaction with its periodic images.[14,18,19] We constructed the structure of amorphous SiO_2 (a-SiO_2), which contains 24 SiO_2 units within the continuous random network (CRN) model with fourfold-coordinated Si and twofold-coordinated O. Starting with randomly distributed 24 Si and 48 O atoms in the given supercell with a fixed experimental density of 2.2 g/cm^3, the oxide system was relaxed via a sequence of bond transpositions using the Metropolis Monte Carlo (MMC) method based on Keating-like interatomic potentials.[18] The a-SiO_2 structure was further refined using DFT calculations (as detailed above). The CRN-MMC approach has been demonstrated to an effective way to determine the fully relaxed structure of a-SiO_2.[14,18,19] We also performed cluster model calculations to evaluate defect energetics under strain-free conditions using the same DFT calculation condition and geometry optimization scheme as for periodic calculations. The values reported below are from periodic DFT calculations unless noted otherwise.

III. RESULTS AND DISCUSSION

A. Structure and energetics of B-related defects

For the sake of reference, we first looked at the minimum-energy configurations of neutral B in crystalline α quartz. As shown in Figs. 1(a)–1(c), three stable states have been identified,[5,6] i.e., (a) trivalent B (TvB or TvB1, see below) with an unpaired electron centered on the adjacent Si atom (=B-$\dot{\text{S}}$i= where – and • represent a Si-O bond and a dangling bond, respectively), (b) divalent B (DvB) (≡Si-$\dot{\text{B}}$-) where an unpaired electron resides on the B atom, and (c) boron-oxygen hole center (BOHC) with a nonbridging O[$\dot{\text{O}}$-B(Si≡)$_2$] which contains an unpaired electron. The DvB and BOHC states are nearly degenerate, and they are predicted to be 0.09 eV less favorable than the TvB state, in good agreement with previous DFT-GGA calculations.[5,6]

Next, we performed a search for possible minimum-energy states for neutral B in amorphous silica (a-SiO_2).

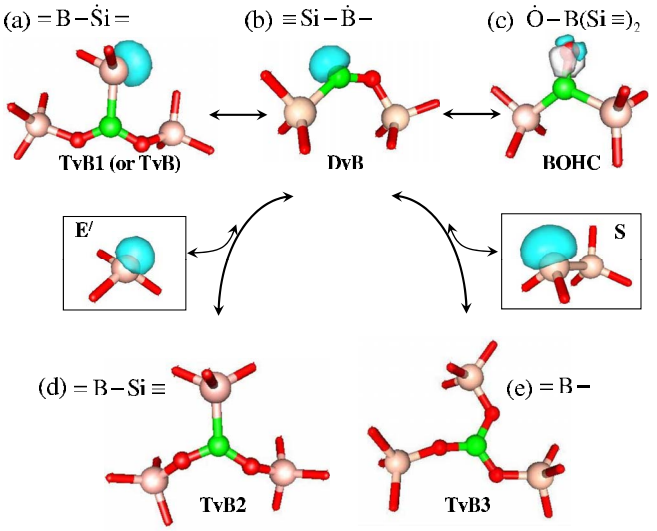

FIG. 1. (Color online) Illustration of the minimum-energy configurations of neutral B in a-SiO_2 and their interconversions mediated by E′ and S centers, (a) trivalent B (TvB or TvB1, see the text) with an unpaired electron centered on the adjacent Si atom (=B-$\dot{\text{S}}$i = where – and • represent a Si-O bond and a dangling bond, respectively), (b) divalent B (DvB) (≡Si-$\dot{\text{B}}$-) where an unpaired electron resides on the B atom, (c) boron-oxygen hole center (BOHC) with a nonbridging O [$\dot{\text{O}}$-B(Si≡)$_2$] which contains an unpaired electron, (d) trigonal BO_2Si (TvB2) where the B atom is linked to two O atoms and one Si atom, and (e) trigonal BO_3 (TvB3) where the B atom is bonded to three O atoms. The interconvertible TvB1, DvB, and BOHC structures are formed upon B interstitial introduction into the defect-free a-SiO_2 matrix, while each of which contains an oxygen vacancy and an unpaired electron, in comparison to the defect-free trigonal BO_3 (TvB3) structure. The unpaired electrons in TvB1, DvB, E′ and S, and the B-O bond and lone electron pairs in BOHC are represented by the maximally localized Wannier functions, which were calculated using the CPMD package (Ref. 20). From the TvB1, DvB, or BOHC states, either an E′ (Ṡi≡) or S (=Ṡi-Si≡) center can be released in a-SiO_2 (which is unlikely in crystalline α quartz), resulting in the TvB2 or TvB3 state as indicated (see also Fig. 2). Small dark (red), small gray (green), and big gray (pink) balls represent O, B, and Si atoms, respectively.

Like in crystalline α quartz, the TvB (=B-$\dot{\text{S}}$i=), DvB (≡Si-$\dot{\text{B}}$-), and BOHC ($\dot{\text{O}}$-B(Si≡)$_2$) states were also identified to be stable. While the defect formation energies significantly vary from site to site due to different local bond topologies in the amorphous matrix, the TvB (=B-$\dot{\text{S}}$i=) state turns out to be the most stable and the DvB (≡Si-$\dot{\text{B}}$-) and BOHC ($\dot{\text{O}}$-B(Si≡)$_2$) states are practically degenerate. The energy gain of TvB over DvB and BOHC is predicted to be 0.8 ± 0.6 eV, which is substantially greater than 0.09 eV in crystalline α quartz. Here, to get good statistics we carefully sampled the defect structures at various locations (about 18 sites) in three different α-SiO_2 supercells considered. To minimize the effect of local strain, we also performed cluster model calculations using $(OH)_2Si$-B(OH)-O-Si$(OH)_3$ and $(OH)_3Si$-B-O-Si$(OH)_3$, which are assumed to mimic the TvB (=B-$\dot{\text{S}}$i=) and DvB (≡Si-$\dot{\text{B}}$-) states, respectively. The cluster

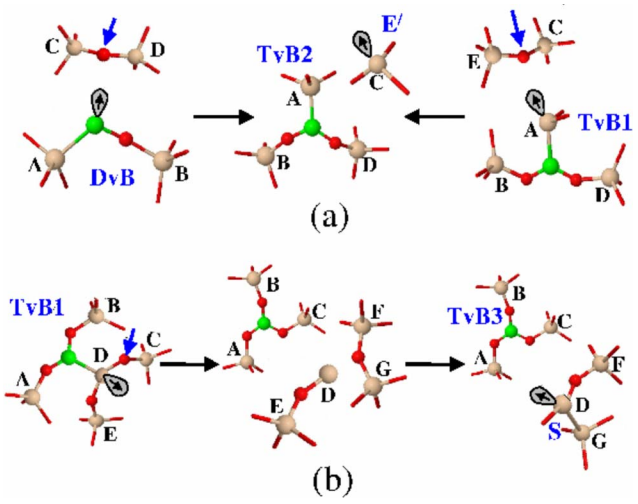

FIG. 2. (Color online) Predicted formation pathways of (a) TvB2 and (b) TvB3 from TvB1 or DvB in a-SiO_2, as indicated. The transformations are unlikely to occur in crystalline α quartz. Small dark (red), small gray (green), and big gray (pink) balls represent O, B, and Si atoms, respectively, and dangling bonds are also indicated. TvB1 is predicted to be 0.09 eV and 0.8 ± 0.6 eV more favorable than DvB in α quartz and a-SiO_2, respectively, while DvB is energetically comparable to BOHC [Fig. 1(c)] in both α quartz and a-SiO_2. In addition, our periodic and cluster DFT calculations show that TvB1, TvB2+E/, and TvB3+S are practically degenerate in energy if they are fully relaxed (see the text).

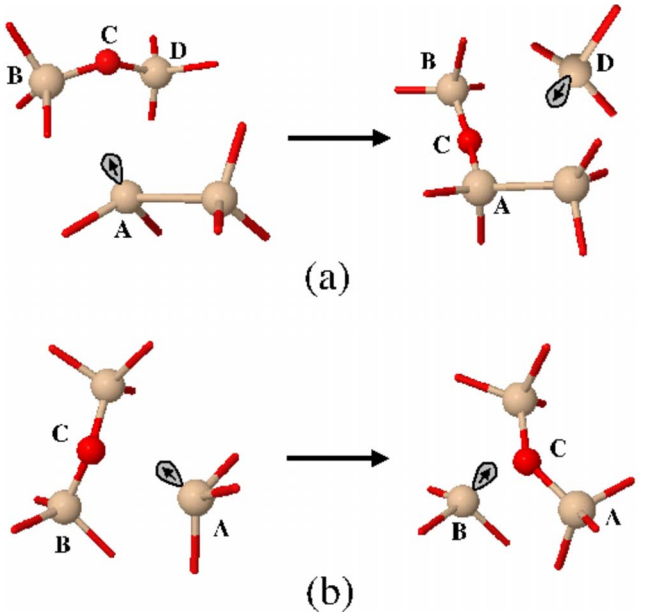

FIG. 3. (Color online) Illustrations of (a) dissociation of an S center into an O vacancy and an E/ center and (b) diffusion of an E/ center in a-SiO_2. Small dark (red) and big gray (pink) balls represent O and Si atoms, respectively, and dangling bonds are also indicated.

calculation result also indicates that the former is 0.79 eV more favorable than the latter, consistent with the periodic calculation result. We attribute the discrepancy between α quartz and a-SiO_2 to the larger strain associate with the rather rigid threefold =B-Ṡi= (TvB) state compared to the twofold ≡Si-Ḃ-(DvB) state in α quartz, while the flexible amorphous matrix renders a well-relaxed TvB structure.

In a-SiO_2, besides TvB (=B-Ṡi=), DvB (≡Si-Ḃ-), and BOHC ($\dot{O}$-B(Si≡)$_2$), our calculations show the formation of trivalent =B-Si≡ and =B-, which is unlikely in crystalline α quartz. Hereafter, we refer to the three different trivalent =B-Ṡi=, =B-Si≡, and =B- states as TvB1, TvB2, and TvB3, respectively. As illustrated in Fig. 1, TvB2 [(d)] and TvB3 [(e)] can be created by releasing E/ (Ṡi≡) and S (=Ṡi-Si≡) centers from TvB1 or DvB. Our calculations suggest the following possible routes for TvB2 and TvB3 formation. For TvB2 (=B-Si≡) [middle panel], as shown in Fig. 2(a), either the Ḃ in ≡Si-Ḃ- [left panel] or the Ṡi in =B-Ṡi= [right panel] reacts with a neighboring lattice O (as indicated) while breaking a Si-O bond (Si_C-O), i.e., ≡Si-Ḃ-+-O-Si≡ → ≡Si-B=+Ṡi≡ or =Ṡi-B=+-O-Si≡ → ≡Si-B=+Ṡi≡. The TvB3 formation may involve a two-step reaction [Fig. 2(b)]: (1) the B in =B-Ṡi= grabs a neighboring lattice O (as indicated by an arrow) linked to the Ṡi [left panel], yielding a monovalent Si (indicated as D) [middle panel], i.e., =B-Ṡi= → =B-+:Ṡi-; and (2) the unstable monovalent Si (D) almost spontaneously evolves into an S defect center by breaking a Si-O bond (Si_G-O) [right panel], i.e., ≡Si-O-+:Ṡi- → ≡Si-Ṡi=. We evaluated the energetics of the interconversions between TvB1, TvB2+E/, and TvB3+S using cluster model calculations, with (OH)$_2$Si-B(OH)-O-Si(OH)$_3$+(OH)$_3$Si-O-Si(OH)$_3$, ((OH)$_3$ Si-O-)Si(OH)$_2$-B(OH)-O-Si(OH)$_3$+(OH)$_3$Si, and (HO)$_2$B-O-Si(OH)$_3$+(OH)$_3$Si-O-Si(OH)-Si(OH)$_3$, which are assumed to mimic =Ṡi-B=+-O-Si≡, =B-Si≡+Ṡi≡, and =B-+=Ṡi-Si≡, respectively. We find that there is practically no change in the total energy, implying that TvB1, TvB2 +E/, and TvB3+S will be degenerate if they are fully relaxed. This is not surprising considering the similar nature of the three defect states which commonly involve trivalent =Ṡi- and -B=. Our extensive periodic calculations also show that their total energies are comparable to each other. For about 18 sample locations in three different a-SiO_2 supercells employed, the most energetically favorable B configuration turns out to be one of the TvB1, TvB2+E/, and TvB3+S states (about 50% in TvB3+S, 30% in TvB1, and 20% in TvB2+E/) depending on local bond topologies. Although the TvB3+S structure tends to be prevailing because it can be more easily relaxed than the TvB1 and TvB2+E/ structures in the amorphous silica matrix, their energy differences are insignificant in most cases. This suggests possible interconversions between TvB1, TvB2, and TvB3 mediated by E/ and/or S centers.

Our periodic calculations show that an S defect center is mobile with a barrier of 1.5 ± 0.6 eV during high-temperature thermal treatment, and may dissociate into an O vacancy and an E/ center by grabbing a nearby lattice O, i.e., =Ṡi-Si≡ → ≡Si-Si≡+Ṡi≡ [Fig. 3(a)]. According to our cluster model calculations [(HO)$_2$Si-Si(OH)$_3$ + (HO)$_3$ Si-O-Si (OH)$_3$ → (OH)$_3$ Si-O-Si (OH)$_2$-Si(OH)$_3$

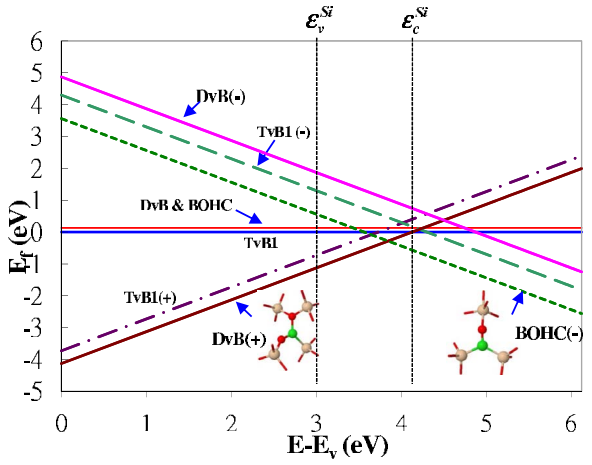

FIG. 4. (Color online) Variation in the relative formation energies of B-related defects with respect to neutral TvB1 in α quartz as a function of Fermi energy for the computed silica gap of 6.2 eV. The minimum-energy configurations of positively charged DvB(+) and negatively charged BOHC(−) are also presented in the insets. The vertical dotted lines indicate the positions of experimental Si valence ($\varepsilon_v^{\mathrm{Si}}$) and conduction ($\varepsilon_c^{\mathrm{Si}}$) bands for a thin silica layer on the Si substrate. More details regarding the band alignment can be found in Ref. 23.

$+(\mathrm{HO})_3\mathrm{Si}$], the dissociation reaction is predicted to be endothermic by about 0.2 eV for their well-relaxed configurations. In addition, we find that an E' undergoes diffusion with a moderate barrier of <1.3 eV [Fig. 3(b)] using periodic calculations, and may convert to O vacancy if it encounters another E' center, i.e., $\equiv\dot{\mathrm{S}}\mathrm{i}+\dot{\mathrm{S}}\mathrm{i}\equiv\rightarrow\equiv\mathrm{Si\text{-}Si}\equiv$. The resulting exothermicity is estimated to be 3.4 eV from a cluster model calculation with $_3(\mathrm{OSiH}_3)\mathrm{Si\text{-}Si}(\mathrm{OSiH}_3)_3$, in good agreement with previous studies.[21] According to the cluster calculations, the relative formation energies of the E' and S centers with respect to an O vacancy are approximated to be 1.7 and 1.5 eV in the neutral state, respectively. More details regarding the behavior of the O vacancy related defects will be presented elsewhere. Allowing E' and S centers to escape from the $=\mathrm{B\text{-}}\dot{\mathrm{S}}\mathrm{i}=$ and $=\mathrm{B\text{-}Si}\equiv$ states, we can expect that B atoms exist preferentially in the trigonal BO_3 structure (=B-, TvB3) in a-SiO_2, which is also well supported by earlier spectroscopy measurements.[22]

We also looked at the formation of B-related defects in different charge states. Earlier theoretical studies[5,6] suggested that in α-quartz B may favor positively or negatively charged states, depending on the electron chemical potential, while exhibiting a negative-U behavior. Figure 4 shows the relative formation energies of TvB1, DvB, and BOHC in different charge states as a function of Fermi level within the computed gap of silica. For a SiO_2 film deposited on the Si substrate, the vertical dotted lines indicate the positions of experimental Si valance and conduction bands, denoted as $\varepsilon_v^{\mathrm{Si}}$ and $\varepsilon_c^{\mathrm{Si}}$, respectively, which were adjusted based on experimental and theoretical energy levels associated with interstitial hydrogen in SiO_2 (which is known to be 0.2 eV higher than the Si midgap at the $\mathrm{Si}/\mathrm{SiO}_2$ system). More details on the band alignment can be found elsewhere.[5,6,23]

In α quartz, as shown in Fig. 4, for the computed gap of 6.2 eV, the positively charged DvB(+) ($\equiv\mathrm{Si\text{-}B}^+\text{-}$) is favored up to a Fermi level of 3.84 eV, after which the negatively charged BOHC(−) ($^-\mathrm{O\text{-}B}(\mathrm{Si}\equiv)_2$) becomes the most favorable state, in good agreement with previous DFT-GGA calculations.[5,6] Note that the charged DvB(+) and BOHC(−) states are about 0.52 and 0.24 eV more favorable than their neutral counterparts near the assumed Si midgap, respectively. As shown in the insets, the positively charged B in DvB(+) favorably interacts with a neighboring lattice O to form a B-O dative bond, while the negatively charged O in BOHC(−) is bonded to a nearby lattice Si (which becomes fivefold coordinated). This in turn leads to stabilization of the DvB(+) and BOHC(−) states, making either of them energetically more favorable than the neutral TvB1 state within the Si gap depending on the Fermi-level position.

In a-SiO_2, our DFT-GGA calculations show that the energy difference between the neutral DvB and positively charged DvB(+) states with Fermi-level position is similar to that in α quartz (as shown above). However, in the a-SiO_2 matrix the formation of stable BOHC(−) (in which the negatively charged O atom is linked to a neighboring Si lattice atom) is hardly seen, due largely to the sparse nature of amorphous bond network. Given that TvB1 is 0.8 eV more stable than DvB ($\equiv\mathrm{Si\text{-}}\dot{\mathrm{B}}\text{-}$), as opposed to 0.09 eV in α quartz, we expect that the neutral TvB1 ($=\mathrm{B\text{-}}\dot{\mathrm{S}}\mathrm{i}=$) state would be favored near the Si midgap, or at least as favorable as the charged DvB(+) state, for a thin a-SiO_2 layer grown on the Si substrate. This trend is indeed seen in our extensive periodic calculations, while there are sizable site-to-site variations in the defect formation energies in the amorphous matrix as well as uncertainty in the computed ionization levels. Our calculations also show that the TvB2+E' and TvB3+S states mostly favor the neutral charge state near the Si midgap.

B. Diffusion and interconversion of B-related defects

For the sake of comparison, we first calculated the diffusion pathways and barriers of B in the positive and neutral charge states in α quartz, starting from the corresponding most stable DvB(+) and TvB1 configurations, respectively, as proposed previously [see Fig. 3 in Ref. 5, note that DvB(+) and TvB1 are, respectively, equivalent to $\mathrm{B}_{\mathrm{ox}}\mathrm{O}_{(3)}$ and $\mathrm{B}_s\mathrm{Si}_{(3)}$]. Our predicted barriers are close to 2.3 and 0.8 eV for the positive and neutral states from previous DFT-GGA calculations.[5,6]

Following the same routes, in a-SiO_2 the overall barrier of 2.6 ± 0.6 eV is predicted for B diffusion in the positive charge state, similar to the α-quartz case. Here we do not consider the negatively charged B since BOHC(−) formation is rather unlikely in a-SiO_2 as pointed out earlier. For the neutral case, as shown in Fig. 5, a viable diffusion path starting from TvB1 ($=\mathrm{B\text{-}}\dot{\mathrm{S}}\mathrm{i}=$) involves a series of reconfigurations, i.e., $=\mathrm{B\text{-}}\dot{\mathrm{S}}\mathrm{i}=(\mathrm{TvB1})\xrightarrow{E_{m1}}\equiv\mathrm{Si\text{-}}\dot{\mathrm{B}}\text{-}(\mathrm{DvB})\xrightarrow{E_{m2}}\dot{\mathrm{O}}\text{-}\mathrm{B}(\mathrm{Si}\equiv)_2(\mathrm{BOHC})\xrightarrow{E_{m3}}\equiv\mathrm{Si\text{-}}\dot{\mathrm{B}}\text{-}(\mathrm{DvB}')\xrightarrow{E_{m4}}=\mathrm{B\text{-}}\dot{\mathrm{S}}\mathrm{i}=(\mathrm{TvB1}')$. The corresponding energy barriers are predicted to be $E_{m1}\approx2.1\pm0.5$ eV, $E_{m2}\approx0.7\pm0.1$ eV, $E_{m3}\approx0.7\pm0.1$ eV, and $E_{m4}\approx1.3\pm0.5$ eV, respectively. Compared to the α-quartz case, the first step barrier (E_{m1}) is higher by

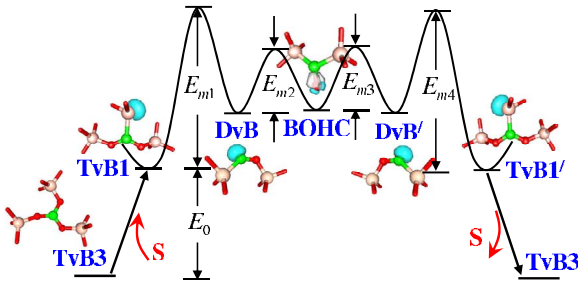

FIG. 5. (Color online) Schematic illustration of the predicted defect-mediated mechanism of B diffusion in a-SiO_2, starting from the most probable trigonal TvB3 state with an S center. The associated B diffusion barriers, E_{m1}-E_{m4}, and the energy cost for S center creation, E_0, are discussed in the text. In the insets, small dark (red) and big gray (pink) balls represent O and Si atoms, respectively, as shown in Fig. 1.

1.3 ± 0.5 eV, which is due to the significant stabilization of TvB1 in a-SiO_2 (see above). The B diffusion may proceed until TvB1 converts to either TvB2 or TvB3, by releasing an $E^/$ or S center, respectively. The energy barriers for the TvB1 $\leftrightarrow$ TvB2 + $E^/$ and TvB1 $\leftrightarrow$ TvB3 + S interconversions are predicted to be 1.0 ± 0.4 eV and 1.35 ± 0.6 eV, respectively, while TvB1, TvB2 + $E^/$, and TvB3 + S are energetically degenerate. Since large activation energies are required to break multiple strong B-O bonds, B atoms in the trivalent TvB2 (=B-Si≡), and TvB3 (=B-) states are rather unlikely to undergo diffusion.

Considering that B atoms preferentially remain in the trivalent TvB3 state in a-SiO_2, B diffusion may require the TvB3 $\rightarrow$ TvB1 conversion by capturing trivalent Si centers such as S and $E^/$. Earlier experiments[24–27] suggested that S centers could be created by oxide decomposition at the Si/SiO_2 interface, and may diffuse into the SiO_2 layer during high-temperature thermal treatment. The S center density appears to increase with annealing temperature, with an activation energy of 1.7 ± 0.4 eV.[26] In addition, during thermal annealing SiO pairs emitted from the Si/SiO_2 interface are likely to diffuse into the SiO_2 layer and favorably convert to O vacancies.[14] While the O vacancies could also be decomposed to create trivalent Si defects, our calculations predict the relative formation energy of S centers with respect to O vacancies to be 1.5 eV (which may need further refinement using bigger cluster models and/or periodic models, but close to 1.7 ± 0.4 eV as observed for S center creation at the Si/SiO_2 interface). In a thin oxide film, point defects generally originate from a reaction at the film boundary, while bulk generation plays a minor role except under nonequilibrium conditions. Irrespective of the S center source, the energy cost for TvB1 (=TvB3 + S) formation appears to be about 1.5–1.7 eV, relative to the most probable TvB3.

Based on the predicted formation energies and diffusion barriers, we postulate a mechanism for B diffusion in a-SiO_2. As illustrated in Fig. 5, B diffusion may begin by forming TvB1, possibly via the reaction of the most probable TvB3 (=B-) defect and an S center. The TvB1 defect could then undergo diffusion by overcoming a barrier of 2.1 ± 0.5 eV. Assuming the S center originates from the Si/a-SiO_2 interface with an energy cost of approximately 1.7 eV, the overall activation energy for B diffusion in the neutral state is estimated to be 3.8 ± 0.5 $(=1.7 + 2.1 \pm 0.5)$ eV. Although there are non-negligible uncertainties in determining the formation energies and diffusion barriers of the B-related defects in various charge states particularly in the amorphous matrix, the predicted activation energy falls well within the range of 3.5–4.0 eV as reported by previous experiments.[4,7,8] Our findings well support the possibility that B diffusion may be mediated by O vacancy related defects, and thus is enhanced with increasing the defect density. This is analogous to Si self diffusion,[28–31] shedding some light on the anomalous correlation of B diffusion and Si self-diffusion in a-SiO_2, as often seen in experiments.[8–11]

IV. SUMMARY

We examined the structure and diffusion of B atoms in a-SiO_2 using spin-polarized DFT calculations within the generalized gradient approximation. Our calculations confirm that incorporation of a boron atom into SiO_2 results in three minimum-energy configurations, such as =B-$\dot{S}$i=(TvB1), where – and • represent a Si-O bond and a dangling bond, respectively, ≡Si-$\dot{B}$-(DvB) and $\dot{O}$-B(Si≡)$_2$(BOHC). While the DvB and BOHC states appear to be nearly degenerate, the energy gain of TvB1 over DvB and BOHC is predicted to be 0.8 ± 0.6 eV in a-SiO_2, substantially greater than 0.09 eV in crystalline α quartz. Note that each of the B-related defects contains an oxygen vacancy and an unpaired electron, in comparison to the defect-free trigonal =B- structure. In the a-SiO_2 matrix, we also find that the TvB1, DvB, and BOHC states can further convert to the trigonal =B-Si≡ (TvB2) and =B- (TvB3) states by releasing trivalent Si defects such as $E^/$ ($\dot{S}$i≡) and S (=$\dot{S}$i-Si≡) centers, which is unlikely in α quartz. According to our periodic and cluster DFT-GGA calculations, the TvB1, TvB2 + $E^/$, and TvB3 + S states are practically degenerate if they are fully relaxed. This suggests their possible interconversions mediated by $E^/$ and/or S centers, while $E^/$ and S centers are predicted to undergo diffusion with barriers of approximately <1.3 and 1.5 ± 0.6 eV, respectively. Given that B atoms preferentially exist in the trigonal BO_3 (TvB3) structure in a-SiO_2, as evidenced by earlier experiments, our work suggests that B diffusion may require transformation of the immobile TvB3 state to the mobile TvB1 state (i.e., =B-+=$\dot{S}$i-Si≡ $\rightarrow$ =B-$\dot{S}$i=) by capturing an S center or equivalent defects, by crossing a barrier of 1.35 ± 0.6 eV. For the neutral charge state, B is predicted to undergo diffusion starting from the TvB1 configuration via a series of reconfiguration processes, by overcoming an overall barrier of 2.1 ± 0.5 eV. We also looked at the B structure and diffusion in different charge states, showing that in a thin a-SiO_2 layer grown on the Si substrate the neural case can be favored near the Si midgap, or at least as favorable as the positively charged case. Taking the experimentally observed

energy cost of 1.7 ± 0.4 eV for S center creation from the Si/SiO_2 interface,[26] the overall activation energy of B diffusion in the neutral state is estimated to be about 3.8 eV, which falls well within the range of 3.5–4.0 eV as reported by previous experiments.[4,7,8] In addition, the present defect-mediated model for B diffusion mediated can explains well the anomalous correlation of B diffusion with Si self-diffusion in a-SiO_2, as the Si diffusion behavior is also mainly determined by oxygen vacancy related defects.

ACKNOWLEDGMENTS

We acknowledge Semiconductor Research Corporation (Grant No. 1413-001), National Science Foundation (Grant No. CAREER-CTS-0449373), and Robert A. Welch Foundation (Grant No. F-1535) for their financial support. We would also like to thank the Texas Advanced Computing Center for use of their computing resources.

*Author to whom correspondence should be addressed; gshwang@che.utexas.edu

[1] J. R. Pfiester, L. C. Parrollo, and F. K. Baker, IEEE Electron Device Lett. **11**, 247 (1990).
[2] J. R. Pfiester, F. K. Baker, T. C. Mele, H.-H. Tseng, P. J. Tobin, J. D. Hayden, J. W. Miller, C. D. Gunderson, and L. C. Parrillo, IEEE Trans. Electron Devices **37**, 1842 (1990).
[3] R. B. Fair, IEEE Electron Device Lett. **17**, 497 (1996).
[4] R. B. Fair, J. Electrochem. Soc. **144**, 708 (1997).
[5] M. Otani, K. Shiraishi, and A. Oshiyama, Phys. Rev. Lett. **90**, 075901 (2003).
[6] M. Otani, K. Shiraishi, and A. Oshiyama, Phys. Rev. B **68**, 184112 (2003).
[7] T. Aoyama, K. Suzuki, H. Tashiro, Y. Toda, T. Yamazaki, Y. Arimoto, and T. Ito, J. Electrochem. Soc. **140**, 3624 (1993).
[8] T. Aoyama, H. Tashiro, and K. Suzuki, J. Electrochem. Soc. **146**, 1879 (1999).
[9] M. Uematsu, H. Kageshima, Y. Takahashi, S. Fukatsu, K. M. Itoh, and K. Shiraishi, Appl. Phys. Lett. **85**, 221 (2004).
[10] M. Uematsu, H. Kageshima, Y. Takahashi, S. Fukatsu, K. M. Itoh, and K. Shiraishi, J. Appl. Phys. **96**, 5513 (2004).
[11] M. Uematsu, H. Kageshima, S. Fukatsu, K. M. Itoh, K. Shiraishi, M. Otani, and A. Oshiyama, Thin Solid Films **508**, 270 (2006).
[12] T. Aoyama, H. Arimoto, and K. Horiuchi, Jpn. J. Appl. Phys., Suppl. **40**, 2685 (2001).
[13] T. Aoyama, K. Suzuki, H. Tashiro, Y. Tada, H. Arimoto, and K. Horiuchi, J. Appl. Phys. **89**, 4570 (2001).
[14] C.-L. Kuo, S. Lee, and G. S. Hwang, J. Appl. Phys. **104**, 054906 (2008).
[15] J. P. Perdew and Y. Wang, Phys. Rev. B **45**, 13244 (1992).
[16] G. Kresse and J. Furthmuller, *VASP the Guide* (Vienna University of Technology, Vienna, Austria, 2001).
[17] D. Vanderbilt, Phys. Rev. B **41**, 7892 (1990).
[18] D. Yu, G. S. Hwang, T. A. Kirichenko, and S. K. Banerjee, Phys. Rev. B **72**, 205204 (2005) references cited therein.
[19] D. Yu and G. S. Hwang, Electrochem. Solid-State Lett. **11**, P17 (2008).
[20] CPMD, Copyright IBM Corp 1990–2001, Copyright MPI für Festkörperforschung Stuttgart 1997–2004.
[21] J. Ushio, K. Nakagawa, M. Miyao, and T. Maruizumi, Phys. Rev. B **58**, 3932 (1998).
[22] K. Kawagishi, M. Susa, T. Maruyama, and K. Nagata, J. Electrochem. Soc. **144**, 3270 (1997).
[23] P. E. Blöchl and J. H. Stathis, Phys. Rev. Lett. **83**, 372 (1999).
[24] A. Stesmans and V. V. Afanas'ev, Appl. Phys. Lett. **69**, 2056 (1996).
[25] A. Stesmans and V. V. Afanas'ev, Phys. Rev. B **54**, R11129 (1996).
[26] A. Stesmans, B. Nouwen, and V. V. Afanas'ev, Phys. Rev. B **66**, 045307 (2002).
[27] A. Stirling and A. Pasquarello, Phys. Rev. B **66**, 245201 (2002).
[28] S. Fukatsu, T. Takahashi, K. M. Itoh, M. Uematsu, A. Fujiwara, H. Kageshima, Y. Takahashi, K. Shiraishi, and U. Gösele, Appl. Phys. Lett. **83**, 3897 (2003).
[29] D. Tsoukalas, C. Tsamis, and P. Normand, J. Appl. Phys. **89**, 7809 (2001).
[30] T. Takahashi, S. Fukatsu, K. M. Itoh, M. Uematsu, A. Fujiwara, H. Kageshima, Y. Takahashi, and K. Shiraishi, J. Appl. Phys. **93**, 3674 (2003).
[31] D. Mathiot, J. P. Schunck, M. Perego, M. Fanciulli, P. Normand, C. Tsamis, and D. Tsoukalas, J. Appl. Phys. **94**, 2136 (2003).